

## ON THE POWER SPECTRA OF THE WIND-FED X-RAY BINARY PULSAR GX 301–2

MAURO ORLANDINI<sup>1</sup>

Scuola Internazionale Superiore di Studi Avanzati, Via Beirut 2, I-34014 Trieste, Italy

AND

G. E. MORFILL

Max-Planck-Institut für Physik und Astrophysik, Institut für Extraterrestrische Physik, D-8046 Garching bei München, Germany

Received 1991 March 15; accepted 1991 August 27

## ABSTRACT

In this paper we develop a phenomenological model of accretion which we apply to the wind-fed X-ray binary pulsar GX 301–2. We assume that the accretion onto the neutron star does not occur from a continuous flux of plasma, but from blobs of matter which are threaded by the magnetic field lines onto the magnetic polar caps of the neutron star. These “lumps” are produced at the magnetospheric limit by magnetohydrodynamical instability, introducing a “noise” in the accretion process, due to the discontinuity in the flux of matter onto the neutron star. We link a physical description of accretion to the statistical description of the “noise” generated in the X-ray emission by the accretion process: namely, a shot noise process with a special response function, the form of which is physically interpreted in terms of processes occurring at the magnetospheric limit. Our model is able to describe the change of slope observed in the continuum component of the power spectra of the X-ray binary pulsar GX 301–2, in the frequency range  $0.01 < f_0 < 0.1$  Hz (Orlandini; Orlandini et al.). The physical properties of the infalling blobs derived in our model are in agreement with the constraints imposed by observations.

*Subject headings:* accretion, accretion disks — binaries: close — pulsars: individual (GX 301–2) — stars: neutron — X-rays: stars

## 1. INTRODUCTION

The X-ray pulsar GX 301–2 (4U 1223–62) is located at celestial coordinates (1950)  $\alpha = 12^{\text{h}}23^{\text{m}}49^{\text{s}}$ ;  $\delta = -62^{\circ}29'37''$  (Dower et al. 1978). It was discovered as an X-ray source by a balloon experiment in 1969 (Lewin et al. 1971; McClintock, Ricker, & Lewin 1971), and it was clearly identified as an X-ray source by *Uhuru* (Forman, Jones, & Tananbaum 1976). Its pulsed emission, with a period of  $\sim 700$  s, was discovered by Experiment C on board *Ariel 5* (White et al. 1976). Its binary nature was shown by a Doppler modulation in the X-ray pulse arrival times (Swank et al. 1976; White, Mason, & Sanford 1978). The optical counterpart of GX 301–2 was identified with the supergiant Wray 977, of spectral class B2 Iae (Vidal 1973; Jones, Chetin, & Liller 1974; Parkes et al. 1980). The presence of intense P Cygni profiles in the hydrogen Balmer line series of Wray 977 (Parkes et al. 1980; Hutchings et al. 1982) clearly indicates the presence of an intense stellar wind, suggesting that the mass-loss rate from the supergiant is greater than  $3 \times 10^{-6} M_{\odot} \text{ yr}^{-1}$ . We can surely affirm that GX 301–2 is a wind-fed X-ray binary system, because the typical radius of a supergiant, of the order of  $30 R_{\odot}$  (Allen 1973), is always much smaller than its Roche lobe radius.

We analyzed 10 medium energy *EXOSAT* observations of GX 301–2 (Orlandini 1990; Orlandini et al. 1990) in order to study the aperiodic component of the X-ray flux coming from this source. We observed a change of slope in the continuum of the power spectrum estimates of the X-ray intensity of GX 301–2 in the frequency range  $0.01 < f_0 < 0.1$  Hz. This feature was present in at least two of the 10 observations we analyzed, independently of the intensity of the source and the time resolution of the data. A similar feature has been reported by

Belloni & Hasinger (1990) in another *EXOSAT* observation which we have not analyzed. In order to clarify this behavior we investigate two related topics.

First, from a physical point of view we develop a phenomenological model of inhomogeneous wind accretion, in which the accretion onto the neutron star does not occur from a continuous flux of plasma, but from blobs of matter which are threaded by the magnetic field lines onto the magnetic polar caps of the neutron star. These “lumps” are *not* the inhomogeneities present in the stellar wind coming from the optical companion (as, for instance, those observed in the two wind-fed pulsars 4U 1538–52 [Orlandini 1990; Robba et al. 1991] and Vela X-1 [Nagase et al. 1986]) but are produced at the magnetospheric radius  $r_m$  by magnetohydrodynamical instability (Arons & Lea 1976a, b). Once formed, these blobs of plasma fall toward the neutron star surface. They are channeled by the magnetic field lines onto the magnetic polar caps, where their kinetic energy is converted into X-ray radiation in the process of deceleration. In the framework of this model, it is easy to understand that a “noise” is introduced in the accretion process, due to the discontinuity in the flux of matter onto the neutron star.

Second, we link this physical description of accretion to a statistical description of the “noise” generated in the X-ray emission by the accretion process. There are several models for inhomogeneous accretion onto neutron stars in the literature (Arons & Lea 1980; Hameury, Bonazzola, & Heyvaerts 1980; Morfill et al. 1984; Demmel, Morfill, & Atmanspacher 1990), essentially developed for explaining the super Eddington luminosity observed in some X-ray pulsars (see, e.g., Nagase 1989). An analysis of the type presented here has been performed for isolated pulsars (Lamb, Pines, & Shaham 1978a, b), in order to obtain information on the internal structure of the neutron star, but to our knowledge it is the first time that a statistical

<sup>1</sup> Present address: NASA/Goddard Space Flight Center, Laboratory for High Energy Astrophysics, Code 666, Greenbelt, MD 20771.

description of the “noise” present in the X-ray flux of an X-ray pulsar has been linked successfully to the physics of the magnetohydrodynamical instabilities at the magnetospheric limit.

In § 2 we develop a statistical model able to describe the presence of an inflexion point in the continuum component of the power spectra of GX 301–2: we describe the incoherent component of the X-ray flux as a shot noise process with a special response function (dependent on two free parameters  $\alpha$  and  $\beta$ ). We further derive some relations between the two free parameters of the model in order to obtain the inflexion point in the observed frequency range. In § 3 the physical scenario of “noisy accretion” is described, by applying the theory of plasma penetration developed in a series of paper by Arons & Lea (Arons & Lea 1976a, b; 1980). In the framework of this theory we derive the physical properties of the “lumps” of matter falling onto the neutron star. Then we combine the physics with the “noisy accretion” scenario, to obtain a general time series of the X-ray flux from the pulsar generated by the discrete blobs falling onto the neutron star (i.e., a shot noise process). We constrain our model with the observed properties of the X-ray pulsar GX 301–2, in order to extract information on the physical parameters of the magnetohydrodynamical instability. We derive numerical values for the two free parameters  $\alpha$  and  $\beta$  and give a physical interpretation of them in terms of processes occurring at the magnetospheric limit. The conclusions are summarized in § 4.

## 2. STATISTICAL DESCRIPTION

In this section we treat the statistical description of power spectra. In particular we compute the power spectrum of a shot noise process with a special response function (see, e.g., Papoulis 1965 for definitions and theorems on the shot noise process), which is able to describe in a simple form and with only two free parameters the change of slope observed in the continuum of the power spectra of GX 301–2. It is important to stress here that our theoretical power spectra do not take into account the effects due to counting statistics, time resolution, and finite observing time (these effects have been evaluated by Sutherland, Weisskopf, & Kahn 1978), but they

are computed only to extract a quantitative information on the behavior of the shape of the spectra. In other words here we will not perform any fit to the observed spectra in order to derive the values of the free parameters. This will be done elsewhere (Orlandini et al. 1991).

Let us suppose that the response function  $h(t)$  has the form

$$h(t) = (A \sin \beta t + B \cos \beta t) \exp(-\alpha t) u(t), \quad (1)$$

where  $u(t)$  is the step function. In § 3 a physical interpretation of this function will be given in terms of physical processes which occur at the magnetospheric limit. The power spectrum of a shot noise process  $s(t)$  with a response function given by equation (1) is

$$S_s(f) = 2\pi\lambda^2 \left( \frac{A\beta + \alpha B}{\alpha^2 + \beta^2} \right)^2 \delta(f) + \lambda \frac{(A\beta + \alpha B)^2 + B^2 f^2}{(\alpha^2 + \beta^2 - f^2)^2 + 4\alpha^2 f^2}, \quad (2)$$

where  $\lambda$  is the average number of events (shots) per unit time, assumed to be time independent, and  $f$  is the frequency.

By studying equation (2) we can easily see that the power spectrum shape changes according to the parameter  $K$ , defined as

$$K \equiv B^2(\alpha^2 + \beta^2)^2 + 2(A\beta + \alpha B)^2(\alpha^2 + \beta^2) - 4\alpha^2(A\beta + \alpha B)^2. \quad (3)$$

If  $K \leq 0$ , then the power spectrum has the typical shape of a shot noise process (see Fig. 1a); when  $K \geq 0$  the shape is completely different, showing a maximum at a given frequency  $f_{\max}$  and an inflexion point (see Fig. 1b).

In the particular case  $A = 0$  (which will be considered from here on), we have that case (a) is achieved if

$$\alpha^4 - 4\alpha^2\beta^2 - \beta^4 \geq 0. \quad (4)$$

The two regions defined in the above expression in the  $\alpha^2$ - $\beta^2$  plane are shown in Figure 2.

The position of the inflexion point in the power spectrum, i.e., the point at which the change of slope occurs, is obtained

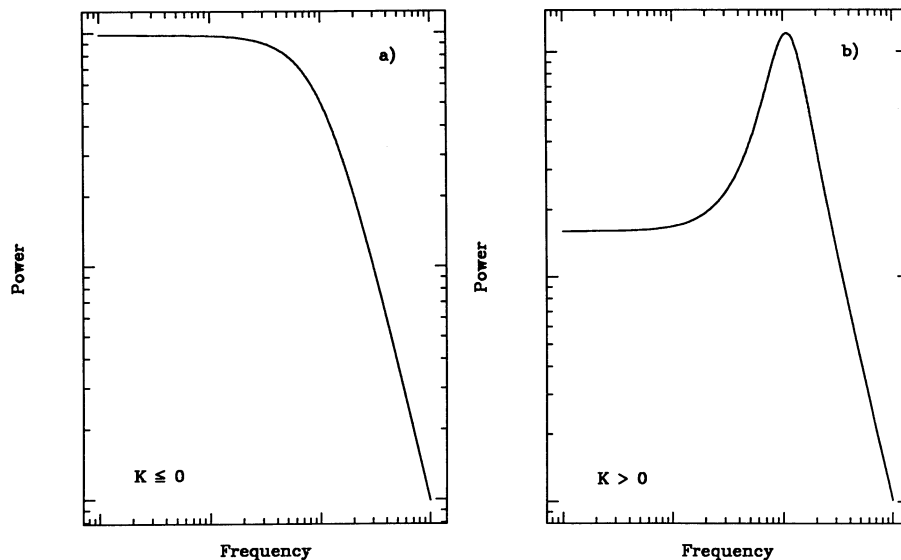


FIG. 1.—Form of the power spectrum of an oscillating exponential shot noise, according to the  $K$  parameter (for simplicity we show here case  $A = 0$ ). Case (a) corresponds to  $K \leq 0$ ; case (b) to case  $K \geq 0$ .

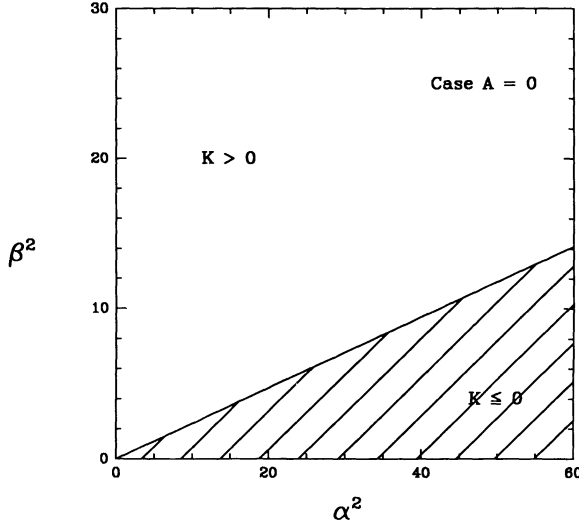


FIG. 2.—The  $\alpha^2$ - $\beta^2$  plane and the two different solutions for the power spectrum shape of an oscillating exponential shot noise with  $A = 0$ . The shaded region corresponds to case  $K \leq 0$ .

by finding the zeros of the second derivative of  $S_s(f)$ . By means of equation (2) we obtain an eighth-order polynomial in  $f$ , in which the coefficients are a function of  $\alpha$  and  $\beta$  (see Appendix, eq. [A2]). To check this model quantitatively we need some physical interpretation of the parameters  $\alpha$ ,  $\beta$ , and  $B$ , and some numerical value for them, in order to find the roots of the polynomial.

In addition, we can obtain a relation between  $\alpha$  and  $\beta$  by imposing the solution  $0.01 < f_0 < 0.1$  Hz in the polynomial in  $f$ . In this way it can be rewritten as a polynomial in  $\beta^2$ , the coefficients of which are a function of the solution  $f_0$  and  $\alpha^2$  (see eq. [A5]). In Figure 3 we show the numerical roots of this

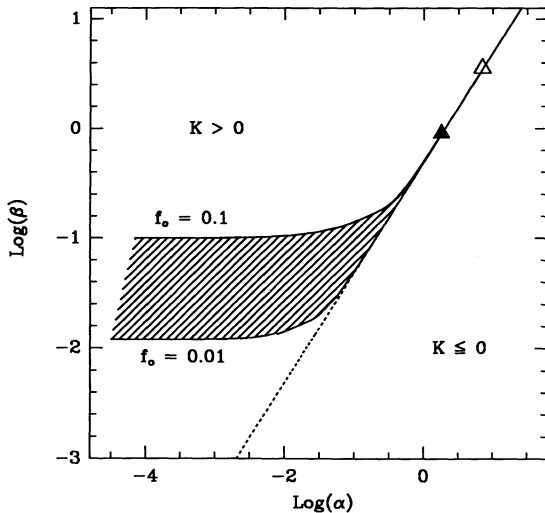


FIG. 3.—Allowed values of  $\alpha$  and  $\beta$  for being in agreement with the observed inflexion point in the GX 301-2 power spectra. The dotted line corresponds to eq. (5), i.e., the relation determining the shape of a power spectrum in our model. The values of  $\alpha$  and  $\beta$  compatible with the observed inflexion point in the GX 301-2 power spectra are shown as a shaded region. Note that, for  $\alpha \geq 1$ ,  $\alpha$  and  $\beta$  converge to the relation of eq. (5). The two triangles indicate the value of  $\alpha$  and  $\beta$ , according to eq. (19), for the two luminosity states of Table 1. The full triangle corresponds to the low state, while the open triangle corresponds to the high state.

polynomial in the  $\alpha$ - $\beta$  plane for  $\alpha$  ranging over seven orders of magnitude, together with the relation of equation (4), corresponding to the two cases  $K \leq 0$ . We can see that for  $\alpha \geq 1$  the allowed values of  $\alpha$  and  $\beta$  compatible with the inflexion point at  $f = f_0$  belong to the curve

$$\beta = \sqrt{5 - 2\alpha} \approx \frac{1}{2}\alpha. \quad (5)$$

For  $\alpha \lesssim 1$  we have a region of allowed solutions (shaded in Fig. 3) but, in both cases, the solutions belong to the  $K > 0$  plane (see Fig. 2).

### 3. PHYSICAL SCENARIO

Let us first describe our physical scenario of discrete accretion onto a neutron star from a stellar wind. The stellar wind coming from the optical companion of the neutron star is captured by its intense gravitational field and accreted. The strong magnetic field halts the incoming matter at a distance of the order of  $r_m \approx 10^8$  cm from the neutron star surface. At a distance of  $\Delta_s$  above  $r_m$  a standoff shock forms; because the magnetosphere is magnetohydrodynamically unstable, plasma can enter in form of filaments of mean length  $\approx \pi r_m (m_0)^{1/2}$ , where  $m_0$  is the mode number which describes the dominant scale height at the equilibrium, defined as (Arons & Lea 1976a)

$$m_0 \equiv b \frac{\mathcal{R}(\theta)}{\Delta_s} \approx 12 L_{37}^{32/35} \mu_{30}^{6/35} m^{-47/35}, \quad (6)$$

where  $b \approx 2$ ,  $\mathcal{R}(\theta)$  is the equilibrium shape of the magnetosphere as a function of the magnetic latitude  $\theta$ ,  $L_{37}$  is the X-ray luminosity in units of  $10^{37}$  ergs  $s^{-1}$ ,  $\mu_{30}$  is the magnetic moment of the neutron star in units of  $10^{30}$  G  $cm^3$ , and  $m$  is the neutron star mass in solar mass units. We have assumed an efficiency  $\epsilon$  of the accretion process, defined as  $\mathcal{L}_x = \epsilon \dot{M}_x c^2$ , equal to 0.2, where  $\mathcal{L}_x$  is the X-ray luminosity,  $\dot{M}_x$  is the accretion rate onto the neutron star, and  $c$  is the speed of light. As shown by Burnard, Lea, & Arons (1983), GX 301-2 satisfies all the requirements because the theory of plasma penetration into the magnetosphere of a wind-fed X-ray binary system is valid, therefore we can apply the detailed theory developed in a series of papers by Arons & Lea (Arons & Lea 1976a, b; 1980).

Once formed, the blobs fall radially toward the neutron star surface. At the beginning Compton cooling is very efficient and therefore the blob temperature is constant, equal to the X-ray temperature. This corresponds to an increase of the blob density  $\rho_b$  as  $r^{-6}$  (we assume a dipolar magnetic field) and a consequent decrease of the blob radius  $r_b$  as  $r^2$ . Assuming a constant mass blob, we have (Arons & Lea 1980; Hayakawa 1985)

$$\begin{aligned} r_b(r) &= \pi \left( \frac{r_m}{m_0} \right) \left( \frac{r}{r_m} \right)^2 \\ &\approx 2.5 \times 10^7 \mu_{30}^{2/5} L_{37}^{-6/5} m^{6/5} \left( \frac{r}{r_m} \right)^2 \left[ \frac{\mathcal{R}(\theta)}{(1 + 3 \sin^2 \theta)^{1/3}} \right] \text{ cm}, \end{aligned} \quad (7)$$

$$\begin{aligned} \rho_b(r) &= \rho_{\text{ff}}(r_m) \frac{v_{\text{ff}}(r_m)}{v_{\text{abs}}(r_m)} \left( \frac{r_m}{r} \right)^6 \\ &\approx 7.6 \times 10^{-10} \mu_{30}^{-27/35} L_{37}^{66/35} m^{-67/70} \left( \frac{r_m}{r} \right)^6 \text{ g cm}^{-3}, \end{aligned} \quad (8)$$

where  $\rho_{\text{ff}}(r_m)$  and  $v_{\text{ff}}(r_m)$  are the free-fall density and velocity,

TABLE 1  
PHYSICAL PROPERTIES OF THE INSTABILITY BLOBS

Low State	High State	Reference
$\mathcal{L}_x \approx 10^{36}$ ergs $s^{-1}$	$\mathcal{L}_x \approx 10^{37}$ ergs $s^{-1}$	
$\dot{M}_x \approx 10^{16}$ g $s^{-1}$	$\dot{M}_x \approx 10^{17}$ g $s^{-1}$	
$r_b(r_m) = 6 \times 10^8$ cm	$r_b(r_m) = 3.7 \times 10^8$ cm	Eq. (7)
$\rho_b(r_m) = 7.2 \times 10^{-12}$ g $cm^{-3}$	$\rho_b(r_m) = 5.5 \times 10^{-10}$ g $cm^{-3}$	Eq. (8)
$M_b = 6.5 \times 10^{15}$ g	$M_b = 1.2 \times 10^{14}$ g	
$r_b(r_p) = 1.1 \times 10^5$ cm	$r_b(r_p) = 7.0 \times 10^3$ cm	Eq. (7)
$\rho_b(r_p) = 1.1 \times 10^{-1}$ g $cm^{-3}$	$\rho_b(r_p) = 8.2 \times 10^{-1}$ g $cm^{-3}$	Eq. (8)
$r_b(r_x) \equiv r_b(r_p)$	$r_b(r_x) \equiv r_b(r_p)$	
$\rho_b(r_x) \equiv \rho_b(r_p)$	$\rho_b(r_x) \equiv \rho_b(r_p)$	
$\alpha_{RT} = (1 - 2/\Gamma)^{-1/2}$	$\alpha_{RT} = (1 - 0.2/\Gamma)^{-1/2}$	Wang & Robertson 1985
$\tau_{RT} = 0.55\alpha_{RT}$ s	$\tau_{RT} = 10.14\alpha_{RT}$ s	Eq. (10)
$\tau_{sq} = 1.2 \times 10^{-5}$ s	$\tau_{sq} = 7.3 \times 10^{-7}$ s	Eq. (11)

We have assumed a magnetospheric radius  $r_m = 6 \times 10^8$  cm and a plasmopause radius  $r_p = 10^7$  cm. The blob mass is assumed constant, and equal to  $4\pi\rho_b r_b^3/3$ .

respectively, evaluated at  $r = r_m$ , and  $v_{abs}$  is the absorption velocity of the plasma at the magnetosphere (Arons & Lea 1980). At the plasmopause the infalling blobs are channeled by the magnetic field lines toward the neutron star polar caps. At this distance particles will exchange angular momentum with the surrounding field by the emission of Alfvén waves (Arons & Lea 1980), leading to the confinement of the motion in a thin skin around the force line.

The last quantities we need are some characteristic time scales. The characteristic time scale for the growth of the Rayleigh-Taylor instability between two fluids of densities  $\rho_{out}$  and  $\rho_{in}$  (with  $\rho_{out} > \rho_{in}$ ) is (Chandrasekhar 1961)

$$\tau_{RT} = \sqrt{\frac{\Lambda}{2\pi g} \left( \frac{\rho_{out} + \rho_{in}}{\rho_{out} - \rho_{in}} \right)}, \quad (9)$$

where  $\Lambda$  is the wavelength of the perturbation and  $g$  is the effective gravitational field. As shown by Wang & Robertson (1985), this time scale can be increased by a factor  $\alpha_{RT}$  due to the magnetic tension at the interface between the two fluids.

We will assume that the outer density  $\rho_{out}$  is a factor  $\Gamma$  higher than the free-fall density at  $r_m$ ; furthermore we apply the Rankine-Hugoniot condition at the jump (Frank, King, & Raine 1985) (the flow is highly supersonic), and we put  $\Lambda \approx r_b(r_m)$ , obtaining

$$\begin{aligned} \tau_{RT} &\approx \alpha_{RT} \sqrt{\frac{5}{6\pi} \frac{r_m^2}{GM_x} r_b(r_m)} \\ &\approx \sqrt{\frac{5}{6\pi} \frac{r_m^2}{GM_x} r_b(r_m) \left( 1 - \frac{\mu^2}{\Gamma} \sqrt{\frac{2}{GM_x} \frac{1}{\dot{M}_x} r_m^{-7/2}} \right)^{-1}}, \quad (10) \end{aligned}$$

where  $G$  is the gravitational constant,  $M_x$  is the neutron star mass, and  $\mu$  is the dipolar magnetic moment of the neutron star.

Another quantity we compute is the time needed for a blob to be squashed onto the neutron star surface, defined as (Morfill et al. 1984; hereafter MO84)

$$\tau_{sq} \equiv \frac{2}{3} \frac{r_x}{v_b(r_x)} \left\{ \left[ \frac{r_x + 2r_b(r_x)}{r_x} \right]^{3/2} - 1 \right\}. \quad (11)$$

Now we have all the elements to compute the physical parameters of the infalling blobs for the X-ray binary pulsar

GX 301–2. The magnetospheric radius for this source is  $r_m = 6 \times 10^8$  cm. We will further assume a plasmopause radius of the order of  $r_p \approx 10^7$  cm. In Table 1 the results are summarized for two different X-ray luminosity states.

At this point we have all the information we need to make a quantitative analysis of our phenomenological model. The first step consists in checking whether our results are in agreement with the observed properties of X-ray pulsars, and in particular with the observed properties of GX 301–2. The first constraint on the physical parameters of the instability blobs derives from the observed pulse-to-pulse variations. The formation rate of the blobs has to be in agreement with the observed luminosity fluctuations. In our model the X-ray luminosity is due to a sum of events  $\mathcal{S}(t)$  that occur randomly (shot noise process)

$$\mathcal{L}_x(t) = \sum_k \mathcal{S}(t - t_k), \quad (12)$$

where  $t_k$  is the time at which the event (shot) occurs. The events occur at an average rate  $\lambda$  (in units of events  $s^{-1}$ ), and the probability that there is an event between  $t$  and  $t + dt$  is given by

$$P(t)dt = \lambda e^{-\lambda t} dt. \quad (13)$$

Because the average number of instability blobs present at the magnetospheric limit is  $(1/2)(4\pi r_m^2/\Lambda^2)$ , we will have that the average rate of shots per unit time is

$$\lambda = \frac{1}{2} \frac{4\pi r_m^2}{\Lambda^2 \tau_{RT}} \approx \begin{cases} 10\alpha_{RT}^{-1} s^{-1} & \text{low state,} \\ 100\alpha_{RT}^{-1} s^{-1} & \text{high state.} \end{cases} \quad (14)$$

These values are to be compared with the observed value of  $\lambda \approx 100 s^{-1}$  (MO84 and Fig. 4). At the light of the uncertainty in  $\alpha_{RT}$  the agreement is good. The factor 1/2 in equation (14) is due to the fact that, at the magnetospheric limit, half of the instability blobs is penetrating the magnetosphere while the other half is rising, on average. Furthermore, because the plasma sustaining the blobs is approach at a rate  $\dot{M}_x$ , by imposing the equilibrium between the amount of matter lost in the boundary layer by Rayleigh-Taylor instability, and the matter replenished in the layer by the incoming stellar wind, we have

$$\dot{M}_x \approx \dot{M}_{RT} \approx \lambda(\Lambda^3 \rho_{out}). \quad (15)$$



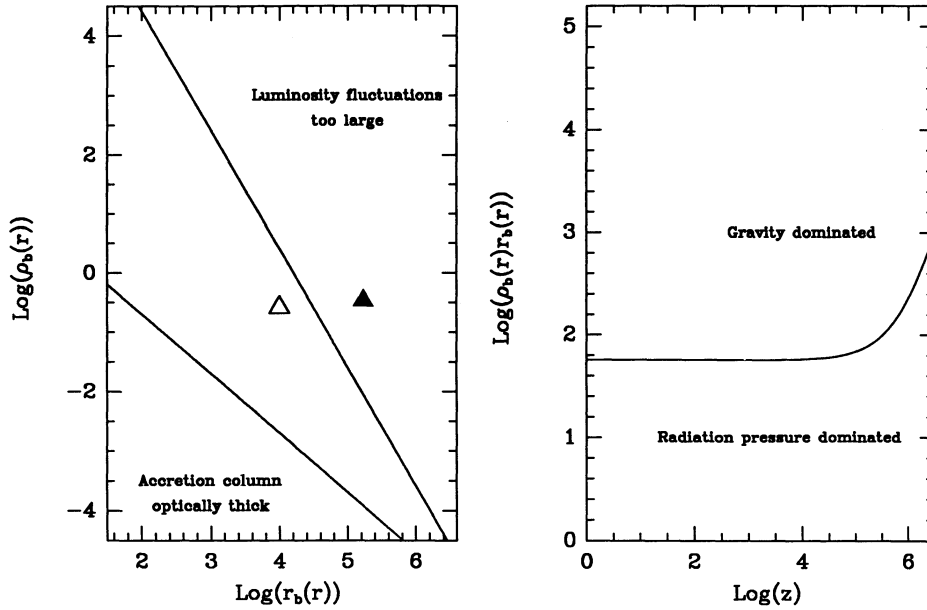


FIG. 4.—Constraints on the physical properties of the instability blobs derived by imposing (a): accretion column is optically thin and pulse-to-pulse variation are not too large (the full triangle corresponds to the low-luminosity state, while the open triangle corresponds to the high-luminosity state); and (b): radiation pressure does not disrupt the infalling blob (MO84). In case (b) the function (momentum transferred from the polar cap)/(gravitational force acting on the blob)  $\equiv 1$  is plotted as a function of the height  $z$  above the neutron star surface. Adapted from MO84.

By combining equations (14) and (15), with the condition  $\rho_{\text{out}} \gg \rho_{\text{in}}$ , we obtain

$$\dot{M}_x \approx \frac{2\pi r_m^2}{\tau_{\text{RT}}} \Lambda \rho_{\text{out}}. \quad (16)$$

The fate of the unstable blobs has been analyzed in great detail by MO84 for the case of accretion from a disk. It is a very interesting coincidence that the blob parameters at the neutron star surface are the same in our model of wind accretion and their model of disk accretion. In this respect some of the MO84 analysis is therefore applicable to our model, too.

MO84 gave some other constraints to the blob physical parameters; in particular they derived a relation between  $r_b$  and  $\rho_b$  by imposing that the accretion column at the magnetic polar cap of the neutron star is optically thin. This requirement is necessary in order that radiation produced by a blob can escape freely without interaction with other falling blobs. In order to have an optically thin accretion column, they derived the relation

$$\rho_b(r_p)r_b(r_p) > \frac{4\dot{M}_x}{\pi^2 r_{\text{cap}} v_b(r_p)} \quad (17)$$

with  $r_{\text{cap}}$  the radius of the polar cap. In the situation considered here, we have substituted the values of blob density and radius at the plasmopause (rather than at the neutron star surface) because, in our model, the unstable blobs fall freely down to  $r_p$  and then are channeled by the magnetic field lines onto the polar caps. The blob properties at the neutron star surface are therefore determined by those at the plasmopause. The second constraint is derived by imposing that the radiation pressure produced by a blob does not disturb and/or disrupt the motion of a subsequent blob. In Figure 4 both the constraints are shown, from which we can see that blobs with  $\rho_b(r_p)r_b(r_p) \gtrsim 50$  can reach the neutron star surface and that radiation pressure is not able to disrupt, on average, an infalling blob (this is valid

even if the blobs are “peeled off” by the radiation pressure [MO84]).

As the last step in our phenomenological model we need to determine a numerical value for  $\alpha$  or  $\beta$  (because the two quantities are related as shown in Fig. 3). One possibility might be to associate the time scale  $\alpha$  with the duration of a single shot. In this case we have an order of magnitude of this time given by  $\tau_{\text{sq}}$  (see eq. [11] and Table 1), and therefore we will have

$$\alpha \approx \tau_{\text{sq}}^{-1} \approx 10^5 - 10^6 \text{ s}^{-1}, \quad (18)$$

where the range for  $\alpha$  corresponds to the two luminosity states discussed in Table 1. While this interpretation seems reasonable, the corresponding time scale  $\beta$ , as inferred from Figure 3, does not find a natural explanation. Furthermore, the physical process associated with  $\alpha$  occurs at the neutron star surface and not at the magnetospheric limit, where the instabilities form. For these reasons we do not favor this particular association of time scales.

A more natural choice would be an association with some physical process which occurs at the magnetospheric limit. The interface between the two fluids, where the Rayleigh-Taylor instability takes place, is not a semi-infinite layer of plasma, but it is sustained by the stellar wind coming from the optical companion. The depletion of the layer could occur in some periodic, quasi-periodic, or chaotic fashion due to (possibly) coherent, self-organized Rayleigh-Taylor instability (see, e.g., Demmel et al. 1990). The characteristic time scale for this process is

$$\tau_{\dot{M}} = \frac{4\pi r_m^2 \Lambda \rho_{\text{out}}}{\dot{M}_x} = 2\tau_{\text{RT}}, \quad (19)$$

where in the last passage we have used equation (16). From equation (19) we can see that the association  $\beta \rightarrow \tau_{\dot{M}}^{-1}$  leads us to associate  $\alpha$  with the time scale  $\tau_{\text{RT}}^{-1}$ . In this way equation (5), derived from the constraints on the inflexion point in the

power spectrum to be in the frequency range  $0.01 < f_0 < 0.1$  Hz, is naturally satisfied and, most important, *both* the processes occur at the magnetospheric limit and their time scales are observable. For these reasons this is our preferred interpretation. The values of  $\alpha$  and  $\beta$  for the two luminosity states of Table 1, obtained from equation (19), are shown in Figure 3.

#### 4. SUMMARY AND CONCLUSIONS

The main goal of this paper was to try to clarify the physics which is hidden in the aperiodic component, the “noisy accretion,” of the X-ray flux coming from X-ray binary pulsars. The observation (Orlandini 1990; Orlandini et al. 1990) of a change of slope in the continuum component of the power spectrum of two GX 301–2 observations, and—most important—the property that the inflexion point is present in the same frequency interval, independently of the X-ray intensity and the time resolution of the data, led us to the development of a statistical model of power spectra, namely a shot noise process with a special response function, of the form

$$h(t) = B \times \underbrace{\cos \beta t}_{\substack{\text{Oscillating} \\ \text{(Replenishment)}}} \times \underbrace{\exp(-\alpha t)u(t)}_{\substack{\text{Exponential} \\ \text{(Depletion)}}, \quad (20)$$

where  $u(t)$  is the step function. Our response function is the product of an “exponential” part and an “oscillating” part, both of them depending on a free parameter. By imposing the position of the inflexion point in the frequency range  $0.01 < f_0 < 0.1$  Hz we obtain the relation between  $\alpha$  and  $\beta$  shown in Figure 3. (It is quite interesting that the same property, i.e., the presence of a “knee” at  $f \simeq 0.1$  Hz, has been observed in the power spectrum of the black hole candidate Cyg X-1 [Nolan et al. 1981], and another X-ray pulsar SMC X-1 [Angelini, Stella, & White 1991].) Next we were able to link the statistical description of power spectra with a physical scenario of inhomogeneous wind accretion. We derived, in the framework of the theory of plasma penetration developed in a series of papers by Arons and Lea (Arons & Lea 1976a, b; 1980), all the physical properties of the instability blobs, both at the magnetospheric radius and at the neutron star surface. These properties are in agreement with the observations. It is interesting to note that the blob properties calculated at the neutron star surface were similar to those obtained for a disk-accretion model (MO84).

Finally, we gave a possible physical meaning to the two free parameters present in the response function: the time scale connected with the “oscillating” part of the response function was related to the time scale induced at the magnetospheric limit by the depletion of the boundary layer in which the Rayleigh-Taylor instability takes place. The time scale connected with the “exponential” part of the response function was related to the rate of formation of the instability blobs. In this way both processes connected with the response function occur at the magnetospheric limit, with time scales of the order of 1 s ( $\tau_M$ ) and  $\frac{1}{2}$  s ( $\tau_{RT}$ ). In other words, the two parts of the response function can be associated with the two opposite effects which control the amount of matter present at any time in the boundary layer: the “exponential” part is connected with  $\tau_{RT}$ , therefore with the depletion of matter from the layer due to Rayleigh-Taylor instability. The “oscillating” part is connected with  $\tau_M$ , therefore with the replenishment of matter in the layer by the stellar wind coming from the optical companion.

Now it remains to explain why the inflexion point is not

present in all the observations of GX 301–2. The two GX 301–2 observations which clearly show the change of slope in their power spectra has been taken at orbital phase  $\phi_{orb} = 0.98$  and  $\phi_{orb} = 0.20$  (we used the ephemeris given by Sato et al. 1986). In the former observation ( $\phi_{orb} = 0.98$ ) the average 1–10 keV X-ray intensity was the highest among all the observations we analyzed, a factor  $\sim 33$  higher than that at  $\phi_{orb} = 0.20$ , in which the intensity was the lowest (Orlandini 1990; Orlandini et al. 1990). Therefore the X-ray intensity (and consequently  $\dot{M}_x$ ) does not seem to play the key role for the presence of an inflexion point. A possible solution to this problem might be connected with equation (15), in which equilibrium between the rate at which matter is pumped in the magnetospheric boundary by the stellar wind and the rate at which matter is expelled from the boundary by Rayleigh-Taylor instability is assumed. Let us consider what occurs when equation (15) does not hold: if  $\dot{M}_x > \dot{M}_{RT}$ , we have that  $\tau_M > 2\tau_{RT}$  and therefore  $\beta < \alpha/2$ . This corresponds, in the  $\alpha$ - $\beta$  plane, to the region  $K < 0$ , where the inflexion point is not present. On the other hand, in the case  $\dot{M}_x < \dot{M}_{RT}$  we will have  $\beta > \alpha/2$  and therefore the presence of an inflexion point (see Fig. 3). Because we expect that the condition  $\dot{M}_x \gtrsim \dot{M}_{RT}$  is more likely than the  $\dot{M}_x \lesssim \dot{M}_{RT}$  condition, in most observations we will not observe an inflexion point in the power spectra. However, there might be some (transient) stages in which the rate at which the stellar wind is accreted is smaller than the rate of depletion of the magnetospheric boundary; for example, when the accretion rate has a sudden decrease, while the Rayleigh-Taylor instability continues to produce instability blobs at the same rate, at the expense of the matter accumulated in the magnetospheric layer. With this interpretation we can explain the lack of correlation between the presence of the inflexion point and the X-ray luminosity. The important property is the *relative* magnitude of  $\dot{M}_x$  with respect to  $\dot{M}_{RT}$  and not its *absolute* value. This explanation is supported by the fact that the two observations having the inflexion point occur at the two extreme X-ray luminosity states (i.e., the brighter and the fainter among all the observations we analyzed), where it is less likely that the balance between  $\dot{M}_x$  and  $\dot{M}_{RT}$  holds.

Another problem, related to the previous one, is the assumed stationarity of the shot noise process, i.e., the dependence of  $\lambda$  with respect to time. This condition is probably unlikely in a strongly variable source such as GX 301–2; therefore a more complete model should take into account the effect of variability of  $\lambda$ , which in turn should be related to the time variability of  $\dot{M}_x$ . Once we have  $\lambda(t)$  it will be possible to write down the analytical form of the power spectrum and compare it to the observed ones.

Our last remark is about the shape of our theoretical power spectra. In computing the power spectrum from our shot noise process we did not compute the effects due to the finite length of the runs and the sampling and integration of the data (this has been done by Sutherland, Weisskopf, & Kahn 1978 for a general shot noise process). Hence we cannot directly fit our theoretical spectra with the observed ones and in this way extract the values of the free parameters of the response function. This is a major data reduction task and it will be done elsewhere (Orlandini et al. 1991). Given the fitting parameters, it will be possible to derive the power spectrum slope, which depends on the four parameters  $\lambda$  (the average number of shot per unit time),  $B$  (the amplitude of the shot),  $\alpha$ , and  $\beta$ , and to search for correlations between these parameters and the physical properties of the GX 301–2 system.

One of us (M. O.) would like to thank Professors D. Dal Fiume and F. Frontera for helpful and stimulating discussions and to acknowledge the warm hospitality of the TESTRE

Institute of Bologna, where part of this work was done. The Italian "Ministero per l'Università e per la Ricerca Scientifica e Tecnologica" is thanked for support.

## APPENDIX

### SEARCH FOR THE INFLEXION POINT IN THE GX 301-2 POWER SPECTRUM

The position of the inflexion point in the power spectrum defined in equation (2), i.e., the point at which the change of slope occurs, is obtained by imposing

$$\frac{d^2 S_s(f)}{df^2} = 0. \quad (\text{A1})$$

In case  $A = 0$ , substituting equation (2) in equation (A1) we obtain an eighth-order polynomial in  $f$ , the coefficients of which are<sup>2</sup> (the odd coefficients are all null)

$$\begin{aligned} \hat{C}_8 &= 3B^2, & \hat{C}_6 &= 2B^2(4\alpha^2 + \beta^2), & \hat{C}_4 &= 6B^2(\alpha^4 - 7\alpha^2\beta^2 - 2\beta^4), \\ \hat{C}_2 &= -6\beta^2 B^2(7\alpha^4 - 2\alpha^2\beta^2 - \beta^4), & \hat{C}_0 &= -B^2(\alpha^2 + \beta^2)^2(\alpha^4 - 4\alpha^2\beta^2 - \beta^4). \end{aligned} \quad (\text{A2})$$

To check this model quantitatively we need some physical interpretation of the parameters  $\alpha$ ,  $\beta$ , and  $B$ , some numerical value for them, to solve the equation

$$\sum_{n=0}^4 \hat{C}_{2n} f^{2n} = 0 \quad (\text{A3})$$

with the coefficients  $\hat{C}_{2n}$  given above (therefore the dependence on  $B$  disappears), and to compare the numerical solution with the observed position of the inflexion point at  $0.01 < f_0 < 0.1$  Hz, obtained from the GX 301-2 power spectra (Orlandini 1990; Orlandini et al. 1990).

On the other hand, we can obtain a relation between  $\alpha$  and  $\beta$  by imposing  $0.01 < f_0 < 0.1$  Hz in equation (A3), which can be rewritten as a polynomial in  $\beta^2$  of the form

$$\sum_{n=0}^4 \hat{B}_n(\beta^2)^n = 0 \quad (\text{A4})$$

with the five coefficients  $\hat{B}_n$ , function of the solution  $f_0$  and  $\alpha^2$ , given by

$$\begin{aligned} \hat{B}_4 &= 1, & \hat{B}_3 &= 6(\alpha^2 + f_0^2), & \hat{B}_2 &= 4(2\alpha^4 + 3\alpha^2 f_0^2 - 3f_0^4), \\ \hat{B}_1 &= 2(\alpha^2 + f_0^2)(\alpha^2 - 22\alpha^2 f_0^2 + f_0^4), & \hat{B}_0 &= -(\alpha^2 - 3f_0^2)(\alpha^2 + f_0^2)^3. \end{aligned} \quad (\text{A5})$$

The numerical solutions of equation (A4) in the  $\alpha$ - $\beta$  plane are shown in Figure 3.

<sup>2</sup> All the analytical computations have been checked with MAPLE (version 4.1, 1987 May), an interactive algebraic manipulator developed by the University of Waterloo, Canada.

## REFERENCES

- Allen, C. W. 1973, *Astrophysical Quantities* (London: Athlone)
- Angelini, L., Stella, L., & White, N. E. 1991, *ApJ*, 371, 332
- Arons, J., & Lea, S. M. 1976a, *ApJ*, 207, 914
- . 1976b, *ApJ*, 210, 792
- . 1980, *ApJ*, 235, 1016
- Belloni, T., & Hasinger, G. 1990, *A&A*, 230, 103
- Burnard, D. J., Lea, S. M., & Arons, J. 1983, *ApJ*, 266, 175
- Chandrasekhar, S. 1961, *Hydrodynamic and Hydromagnetic Stability* (Oxford: Oxford Univ. Press)
- Demmel, V., Morfill, G., & Atmanspacher, H. 1990, *ApJ*, 354, 616
- Dower, R. G., Apparao, K. M. V., Bradt, H. V., Doxsey, R. E., Jernigan, J. G., & Kulik, J. 1978, *Nature*, 273, 364
- Forman, W., Jones, C., & Tananbaum, H. 1976, *ApJ*, 206, L29
- Frank, J., King, A. R., & Raine, D. J. 1985, *Accretion Processes in Astrophysics* (Cambridge: Cambridge Univ. Press)
- Hameury, J. M., Bonazzola, S., & Heyvaerts, J. 1980, *A&A*, 90, 359
- Hayakawa, S. 1985, *Phys. Rep.*, 121, 318
- Hutchings, J. B., Crampton, D., Cowley, A. P., & Bord, D. J. 1982, *PASP*, 94, 541
- Jones, C. A., Chetin, T., & Liller, W. 1974, *ApJ*, 190, L1
- Lamb, F. K., Pines, D., & Shaham, J. 1978a, *ApJ*, 224, 969
- . 1978b, *ApJ*, 225, 582
- Lewin, W. H. G., McClintock, J. E., Ryckman, S. G., & Smith, W. B. 1971, *ApJ*, 166, L69
- McClintock, J. E., Ricker, G. R., & Lewin, W. H. G. 1971, *ApJ*, 166, L73
- Morfill, G. E., Trümper, J., Bodenheimer, P., & Tenorio-Tangle, G. 1984, *A&A*, 139, 7 (MO84)
- Nagase, F. 1989, *PASJ*, 41, 1
- Nagase, F., Hayakawa, S., Sato, N., Masai, K., & Inoue, H. 1986, *PASJ*, 38, 547
- Nolan, P. L., Gruber, D. E., Matteson, J. L., Peterson, L. E., Rothschild, R. E., Doty, J. P., Levine, A. M., Lewin, W. H. G., & Primini, F. A. 1981, *ApJ*, 246, 494
- Orlandini, M. 1990, Ph.D. thesis, International School for Advanced Studies, Trieste
- Orlandini, M., Da Fiume, F., Frontera, F., Robba, N. R., & Busetta, M. C. 1990, *Proc. V GIFCO Congress, San Miniato di Pisa, 1990*, Nov. 28-30, in press
- . 1991, in preparation
- Papoulis, A. 1965, *Probability, Random Variables, and Stochastic Processes* (New York: McGraw-Hill)
- Parkes, G. E., Mason, K. O., Murdin, P. G., & Culhane, J. L. 1980, *MNRAS*, 191, 547
- Robba, N. R., Cusumano, G., Orlandini, M., Dal Fiume, F., & Frontera, F. 1991, *ApJ*, submitted
- Sato, N., Nagase, F., Kawai, N., Kelley, R. L., Rappaport, S., & White, N. E. 1986, *ApJ*, 304, 241
- Sutherland, P. G., Weisskopf, M. C., & Kahn, S. M. 1978, *ApJ*, 219, 1029
- Swank, J. H., Becker, R. H., Boldt, E. A., Holt, S. S., Pravdo, S. H., Rothschild, R. E., & Serlemitsos, P. J. 1976, *ApJ*, 209, L57
- Vidal, N. V. 1973, *ApJ*, 186, L81
- Wang, Y. M., & Robertson, J. A. 1985, *ApJ*, 299, 85
- White, N. E., Mason, K. O., Huckle, H. E., Charles, P. A., & Sanford, P. W. 1976, *ApJ*, 209, L119
- White, N. E., Mason, K. O., & Sanford, P. W. 1978, *MNRAS*, 184, 67P